2012-0386

50th AIAA Aerospace Sciences Meeting including the New Horizons Forum and Aerospace Exposition, 09 - 12 January 2012, Nashville, Tennessee

Surface Integral Analogy Approaches to Computing Noise Generated by a 3D High-Lift Wing Configuration

Hua-Dong Yao[1][*] , Lars Davidson[1][†] , Lars-Erik Eriksson[1][‡]

Olof Grundestam[2][§] , Shia-Hui Peng[1,2][¶] & Peter E. Eliasson[2][‖]

1. Chalmers University of Technology, SE-412 96 Gothenburg, Sweden

2. Swedish Defence Research Agency (FOI), SE-164 90 Stockholm, Sweden

Three surface integral approaches of the acoustic analogies are studied to predict the noise from a three-dimensional, high-lift wing configuration. The approaches refer to the Kirchhoff method, the Ffowcs Williams and Hawkings method of the permeable integral surface and the Curle method. The first two approaches are used to compute the noise generated by the core flow region where the energetic structures exist. The last approach is adopted to predict the noise specifically from the pressure perturbation on the wall. A new way to construct the integral surface that encloses the core region is proposed for the first two methods. Considering the local properties of the flow around the complex objective − the actual wing with high-lift devices − the integral surface based on the vorticity is constructed to follow the flow structures. The noise from the core flow region is based on the dependent integral quantities, which are indicated by the Kirchhoff formulation and by the FWH formulation. The role of each wall component on noise contribution is analyzed using the Curle method. The results of the three methods are then compared.

I. Introduction

The acoustic analogy in computational aeroacoustics (CAA) is used to isolate the noise computation from the computation of the flow that generates the noise. The analogy method was first proposed by Lighthill,[1,2] and it is used to predict the noise of the flow in the free space through the volume integration of the Lighthill stress tensor, T_{ij}. The method was generalized to include the effect of the stationary wall within the flow by Curle.[3] Later, Ffowcs Williams and Hawkings[4] expanded it to flows with moving walls. In both the Curle formulation and the classical FWH formulation, the contribution of the solid wall to noise is derived in the form of integrals over the wall. However, the volume integration of T_{ij} over the surrounding space outside the walls is still needed to predict the noise induced by the flow surrounding the wall. The volume integral limits the application of these methods in practice because of its high computation cost.

To eliminate the need of computing the volume integral, the application of the classical FWH formulation was developed into the form of integrals over a permeable surface instead of a solid body surface.[5,6] The term of the volume integral can be neglected if the permeable surface is considered to enclose most of the sources in the flow field. This method has been validated numerically, for instance, through predicting the noise from helicopter rotors.[5,6] The Kirchhoff method is an alternative acoustic analogy of the surface

---

[*]Department of Applied Mechanics, huadong@chalmers.se

[†]Department of Applied Mechanics, lada@chalmers.se

[‡]Department of Applied Mechanics, lars-erik.eriksson@chalmers.se

[§]Department of Aeronautics and Systems Technology, olof.grundestam@foi.se

[¶]Department of Aeronautics and Systems Technology, shia-hui.peng@foi.se

[‖]Department of Aeronautics and Systems Technology, peter.eliasson@foi.se

integral.[7–10] The integral surface in this method should be located in the linear region of the flow where the wave propagation condition is fulfilled. Then it is necessary to enclose all nonlinear sound sources by the integral surface. The applications of the Kirchhoff method have been discussed in the literature.[11–13] Contrary to the Kirchhoff method, the analytical solution of the FWH method involves the nonlinear effects on and outside the integral surface.[6,14,15] The differences have been evaluated numerically to predict the noise from, for example, helicopter rotors[5,6,15] and jets.[16]

The noise sources of high-lift wings can be categorized into: the trailing edge of the wing, the high-lift devices – the flaps and slats – and their brackets, and the gaps such as the side edge gap between the flap and the wing etc.[17] The trailing edge noise has been studied using the analogy methods,[18,19] theoretical models[20–23] and numerical techniques.[24–26] The slat noise was investigated numerically.[27,28] The gap noise of the last category has been studied by modeling the gap between the flap and the wing,[29] and the trailing edge with the detached flap.[19] In addition to the work above, the noise from a profile of a high-lift wing with a narrow spanwise extent was computed using the FWH method of the permeable integral surface.[28,30,31]

In the current work, the high-lift wing configuration – Config. 2 defined in a companion paper[32] – is employed to study the surface integral approaches including: 1) the Kirchhoff method, 2) the FWH method of the permeable surface and 3) the Curle method. All of the dominant sources as described above will be included in the present computation except the brackets of the high-lift devices.

The integral surface for the Kirchhoff method and the FWH method is defined to follow the characteristics of the flow field. The physics of noise generation is analyzed based on the integration terms of the Kirchhoff equation and the FWH equation, respectively. The noise contributed by the pressure of perturbations on the walls is then studied by the Curle method. Furthermore, the efficiencies of the three approaches in predicting the high-lift wing noise are evaluated.

II.   Methodologies of Surface Integral Acoustics Analogies

II.A.   Formulations of Analogy Methods

II.A.1.   The Kirchhoff Method

By assuming the wave propagation condition to be satisfied outside a stationary surface, the classical Kirchhoff equation is found as:

$$\Box^2 p'\left(\overrightarrow{x},t\right) = -\frac{\partial p'}{\partial n}\delta\left(f\right) - \frac{\partial}{\partial x_i}\left[p'n_i\delta\left(f\right)\right]$$
$$\equiv Q_{KIR}$$

(1)

where n_i denotes the components of the unit outward normal vector to the integral surface, $f(\vec{y}) = 0$ denotes the integral surface that encloses the sound sources, $\Box^2$ is the wave operator and $\delta(f)$ is the Dirac delta function. Using the Green function to Eq. (1), the solution reads:[11]

$$p'_{total,K}\left(\vec{x},t\right) = \frac{1}{4\pi}\int_{f=0}\left\{\frac{\cos\theta}{R^2}\left[p'\left(\vec{y},\tau\right)\right]_{ret} - \frac{1}{R}\left[\frac{\partial p'\left(\vec{y},\tau\right)}{\partial n}\right]_{ret}\right. \\ \left. + \frac{\cos\theta}{c_0 R}\left[\frac{\partial p'\left(\vec{y},\tau\right)}{\partial \tau}\right]_{ret}\right\}dS$$

(2)

where R denotes the modulus of $\vec{r}$, $\vec{r} = \vec{x} - \vec{y}$, $\vec{n}$ is the vector normal to the integral surface, $\cos\theta = (r_i/R)n_i$, c_0 is the speed of sound and the terms in brackets marked by the subscript 'ret' are evaluated at the retarded time $\tau = t - R/c_0$.

The integrations of the sources in Eq. (2) can be interpreted as dependent quantities of the fluctuation, the gradient and the time derivative of the pressure over the integral surface. Hence, the total noise, $p'_{total,K}$, is studied as follows:

$$p'_{1,K}\left(\vec{x},t\right) = \frac{1}{4\pi}\int_{f=0}\left\{\frac{1}{R^2}\cos\theta\left[p'\left(\vec{y},\tau\right)\right]_{ret}\right\}dS$$

(3a)

$$p'_{2,K}\left(\vec{x},t\right) = -\frac{1}{4\pi}\int_{f=0}\left\{\frac{1}{R}\left[\frac{\partial p'\left(\vec{y},\tau\right)}{\partial n}\right]_{ret}\right\}dS$$

(3b)

$$p'_{3,K}\left(\vec{x},t\right) = \frac{1}{4\pi}\int_{f=0}\left\{\frac{1}{R}\frac{\cos\theta}{c_0}\left[\frac{\partial p'\left(\vec{y},\tau\right)}{\partial \tau}\right]_{ret}\right\}dS$$

(3c)

II.A.2.   The FWH Method of the Stationary Permeable Integral Surface

The FWH equation of the stationary permeable integral surface can be treated as a specific case of the moving permeable surface, in which $v_n = 0$. Based on the generalized formulation derived by previous research,[5,6] the specific form is written as

$$\Box^2 p'\left(\overrightarrow{x},t\right) = -\frac{\partial}{\partial x_i}\left[\left(p'\delta_{ij} + \rho u_i u_j\right)n_j\delta\left(f\right)\right]$$
$$+ \frac{\partial}{\partial t}\left[\rho u_j n_j\delta\left(f\right)\right] \tag{4}$$
$$+ \frac{\bar{\partial}^2}{\partial x_i\partial x_j}\left[T_{ij}H\left(f\right)\right]$$

where δ_{ij} is the Kronecker delta, the Lighthill stress tensor is $T_{ij} = (p' - \rho'c_o^2)\delta_{ij} - \tau_{ij} + \rho u_i u_j$ and the bar over the derivative sign denotes the generalized derivative.[14] The viscous terms, τ_{ij}, are neglected in the present analysis.

By assuming the permeable surface to enclose the core flow region, the volume integration for T_{ij} in the solution of Eq. (4) is neglected. Then, its solution reads:

$$p'_{total,F}\left(\vec{x},t\right) = -\frac{1}{4\pi}\frac{\partial}{\partial x_i}\int_{f=0}\left\{\frac{1}{R}\left[p'\delta_{ij} + \rho u_i u_j\right]_{ret}n_j\right\}dS$$
$$+ \frac{1}{4\pi}\frac{\partial}{\partial t}\int_{f=0}\left\{\frac{1}{R}\left[\rho u_j n_j\right]_{ret}\right\}dS \tag{5}$$

The form of Eq. (5) is the same as the solution of the basic FWH equation,[4] in which the wall is used as the integral surface. The first and second integrals in the basic formulation represent the loading noise and the thickness noise, respectively, but they do not have the same physical meaning here. In order to analyze Eq. (5), it is derived as three components:

$$p'_{1,F}\left(\vec{x},t\right) = \frac{1}{4\pi}\int_{f=0}\left\{\frac{1}{R}\cos\theta\left[\left(\frac{1}{c_0}\frac{\partial}{\partial\tau} + \frac{1}{R}\right)p'\right]_{ret}\right\}dS \tag{6a}$$

$$p'_{2,F}\left(\vec{x},t\right) = \frac{1}{4\pi}\int_{f=0}\left\{\frac{1}{R}\lambda_{ij}\left[\left(\frac{1}{c_0}\frac{\partial}{\partial\tau} + \frac{1}{R}\right)(\rho u_i u_j)\right]_{ret}\right\}dS \tag{6b}$$

$$p'_{3,F}\left(\vec{x},t\right) = \frac{1}{4\pi}\int_{f=0}\left\{\frac{1}{R}n_j\left[\frac{\partial}{\partial\tau}(\rho u_j)\right]_{ret}\right\}dS \tag{6c}$$

where $\lambda_{ij} = (r_i/R)n_j$. The noise sources are implied in the equations as the perturbations of the pressure, momentum and mass through the surface.

II.A.3.   The Curle Method for the Turbulent Boundary Layer

The Curle equation generalizes the Lighthill equation[1] to the case in which rigid walls exist in the flow field. For rigid walls, it yields[3,33]

$$\Box^2 p'\left(\overrightarrow{x},t\right) = -\frac{\partial}{\partial x_i}\left[p'n_i\delta\left(f\right)\right] + \frac{\bar{\partial}^2}{\partial x_i\partial x_j}\left[T_{ij}H\left(f\right)\right]$$
$$\equiv Q_{CUR} \tag{7}$$

Its solution is given by[3,33,34]

$$p'_C\left(\vec{x},t\right) = -\frac{1}{4\pi}\frac{\partial}{\partial x_i}\int_{f=0}\left\{\frac{1}{R}\left[p'\right]_{ret}n_i\right\}dS$$
$$+ \frac{1}{4\pi}\frac{\partial}{\partial x_i\partial x_j}\int_V\left\{\frac{1}{R}\left[T_{ij}\right]_{ret}\right\}dV \tag{8}$$

American Institute of Aeronautics and Astronautics Paper 2012-0386

The first integral term in Eq (8) corresponds to the noise induced by the pressure perturbation in the boundary layer flow over rigid walls. This is our interest in the present analysis. Thus the volume integral term of the Lighthill stress tensor, T_{ij}, is neglected. Then, Eq. (8) is rewritten as

$$p'_{total,C}(\vec{x},t) = -\frac{1}{4\pi} \int_{f=0} \left\{ \frac{1}{R} \cos\theta \left[\left(\frac{1}{c_0} \frac{\partial}{\partial \tau} + \frac{1}{R} \right) p' \right]_{ret} \right\} dS \tag{9}$$

II.B.   Comparison of the Analogy Methods

Comparisons have been made of the Kirchhoff method and the FWH method analytically and numerically.[5, 6] Utilizing the continuity and momentum equations, Eq. (4) of the FWH formulation for the stationary permeable surface $(v_n = 0)$ can be rewritten as:[6]

$$\begin{aligned}
\Box^2 p'(\vec{x},t) =& Q_{KIR} \\
& - \frac{\partial}{\partial x_j} \left[\rho u_i u_j \right] n_i \delta(f) - \frac{\partial}{\partial x_j} \left[\rho u_i u_j n_i \delta(f) \right] \\
& + \frac{\bar{\partial}^2}{\partial x_i \partial x_j} \left[T_{ij} H(f) \right]
\end{aligned} \tag{10}$$

This means that there are three additional nonlinear source terms that are considered in the stationary and permeable form of the FWH formulation, comparing with the sources Q_{KIR} in the stationary form of the Kirchhoff formulation. As stated above in Eq. (5), the volume integral of T_{ij} is neglected in our computations, thus limiting the discussions of the differences between the two methods in this paper to the two surface integral terms, which are related to $\rho u_i u_j$ on the integral surface.

As implied by the FWH equation, the permeable surface can be attached onto the walls.[6] Under the preconditions that the wall is stationary with $v_n = 0$, Eq. (10) is transferred to:

$$\Box^2 p'(\vec{x},t) = Q_{CUR} \tag{11}$$

The form of the Curle equation is obtained. It implies that the permeable surface form of the FWH equation, neglecting the volume integral term, accounts for not only the surface sources on the walls in the Curle equation but also the volume sources enclosed in the integral surface.

II.C.   Definition of The Integral Surface

An integral surface needs to be defined in the near-field for integrations when the Kirchhoff method and the FWH method are applied. Here the Curle method will not be discussed because, by definition, its integral surface is the rigid wall. There are two aspects to consider when determining the surface: (1) the distance away from the the walls or the intensive flow area and (2) the geometry constructed.

In the Kirchhoff method, the integral surface is assumed to be located in a position where the condition of the wave propagation is satisfied.[7] In practice, this means that the nonlinear quantities such as $\rho u_i u_j$ on the integral surface must be considerably weaker than the linear terms p', dp/dn and dp/dt.[6] The surface is required to be large enough to enclose most of the strong nonlinear structures of the flow. However, it is challenging to keep the accuracy of the numerical solution on the surface free from numerical contaminations, for example, the dissipation and the dispersion that are caused by the numerical scheme. Therefore, the application of the Kirchhoff method is restricted in practice, although its feasibility in aeroacoustics has been verified.[11, 12, 35] As shown in Eq (10), the FWH method for the permeable surface takes the nonlinear effects into account. This is an advantage since it brings less limitation on the location of the surface.[6, 14, 15] The surface can be placed in the area where nonlinear effects exist. That is, the distance can be closer to the walls or the intensive flow area in the FWH method than the Kirchhoff method.

Continuous and regular geometries are usually chosen to construct the integral surface for the benefit of integrations. For instance, they are designed to be cubic [16] or of the shape of a bottle[36, 37] for a jet, cubic[10] or cylindrical[6, 15] for a helicopter rotor, of a C-shape for an airfoil[38] and cylindrical for a circular cylinder.[31] However, the surface of a regular geometry is not applicable for the high-lift wing, for which the flow field is complex with apparent local structures such as the vortex shedding at the cavity of the main wing and at the kink. The distance between the integral surface and the locally intensive flow region varies independently based on the strength and scale of the local flow structures. Unnecessary extended distance gives rise to

American Institute of Aeronautics and Astronautics Paper 2012-0386

additional computation cost and numerical errors in the solution on the integral surface. Thus the surface is constructed according to the local characteristics of the flow for the high-lift wing.[28, 30, 31]

Even though the surface construction attempts to fit the local characteristics of the flow, it is in practice difficult to make a reasonable geometry artificially. Thus, it is proposed that the surface is built based on the actual properties of the local flow. The vorticity magnitude is employed in the present studies because of its function to indicate the features of flow structures. Because the integral surface is expected to be stationary but capable of enclosing most of instantaneous structures, we take a time-averaged flow field as reference, which can be calculated using RANS.

The integral surface is open at its downstream extremity, to reduce the artificial noise caused by undamped vortices crossing the end of the surface.[38] Similar treatment is reported in the literature on jet noise.[12, 39] However, it results in inaccurately predicted noise in the downstream direction.

III. Application to a Low-Noise High-Life Wing Configuration

The three analogy methods are applied to assess the aeroacoustic performance of a wing configuration with low-noise and high-lift devices, which is referred to as 'Config. 2' in our companion paper.[32] Its geometry is displayed in Fig. 1. As shown in subfigure (a), it consists of a wing and a single slotted flap. The wing has a trailing edge kink and the high-lift system of the flap has separate elements inboard and outboard of the kink. Subfigure (b) shows a cut span-wise plane. There are cavities for all flaps.

(a) Diagram of components

(b) A cut span-wise plane

Figure 1. Sketches for the geometry of Config. 2

III.A. Simulation for the Flow Field

The configurations are attached to a fuselage body in the numerical simulations. A three-dimensional picture for the configuration is shown in Fig. 2. It operates at stall with the highest lift. The basic flow conditions are as follows: the Mach number of the freestream flow is 0.2, and the Reynolds number is 1.7×10^7. The instantaneous quantities of the flow are obtained using a hybrid method of RANS and LES.[40] However, a precursor computation of vorticity is done by RANS for the purpose of searching for an integral surface, which is needed in the Kirchhoff method and the FWH method. The computational domain is spherical with a radius of about 80 times the wing chord. Characteristic boundary conditions are used on the surface of the sphere. To reduce the computational cost, a symmetrical boundary condition is applied at the symmetrical plane at the fuselage. Details on the flow computations can be found in our companion paper.[41]

III.B. Settings in Aeroacoustics Calculation

A rough estimate of voriticity is obtained using a precursor RANS computation. After an isosurface of the vorticity magnitude is found, it is smoothed by computer-aided design (CAD) techniques to become the integral surface. Figure 3 shows the smoothed integral surface and the airframe configuration at three views. The integral surface is compared to three isosurfaces of the dimensionless magnitude of the instantaneous vorticity from the LES-RANS simulation in Fig. 4. The dimensionless vorticity magnitude is given by
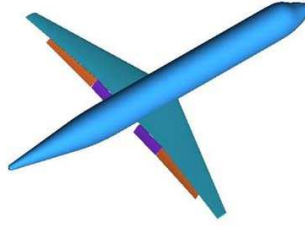
American Institute of Aeronautics and Astronautics Paper 2012-0386

Figure 2. The 3D geometry in numerical simulations

$\overline{w} = |\overrightarrow{w}|L/U$, where $\overrightarrow{w}$ is the vorticity vector, L is the characteristic length of the chord and U is the velocity of the free-stream mean flow. The integral surface ends at 5.5 wing chords downstream of the trailing edge of the flap. It is divided into six colorful parts according to the partition strategy in the surface construction. As shown in Fig. 4(a), the region of dimensionless vorticity magnitudes larger than 2.682 is covered well by the integral surface. When the magnitude decreases to 0.536 in Fig. 4(b), most of the isosurface is covered. For an even further small magnitude 0.268 in Fig 4(c), it is observed that many structures appear out of the integral surface. However, the vorticity is expected to be weak enough with $\overline{w} = 0.536$, and thus the integral surface encloses the core region the flow.

The reference frame for the observers is defined on the basis of the center of the wing root. The observers are placed in a circle on the symmetric plane of the fuselage. The distance from the origin of the frame is 15 times the length of the wing span. The polar axis points to the upstream direction of the mean flow when estimating directivity of the noise. This means that $\theta = 0^o$ is located in the upstream direction, and 180° in the downstream direction. Consequently, 90° and 270° are positioned in the upwards direction and the downwards direction, respectively.

| (a) Bottom view | (b) Side view | (c) Top view |
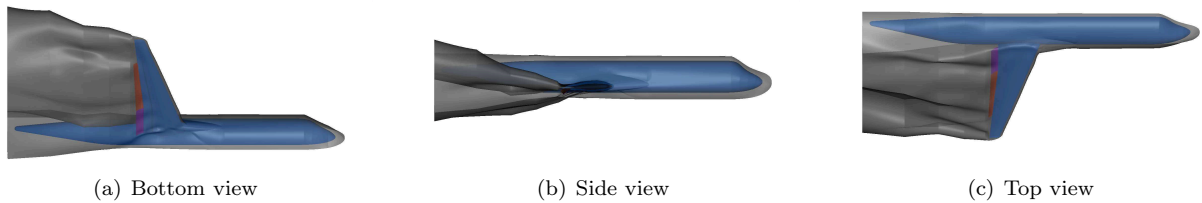
Figure 3. Sketches of the geometry of the integral surface, compared with the airframe

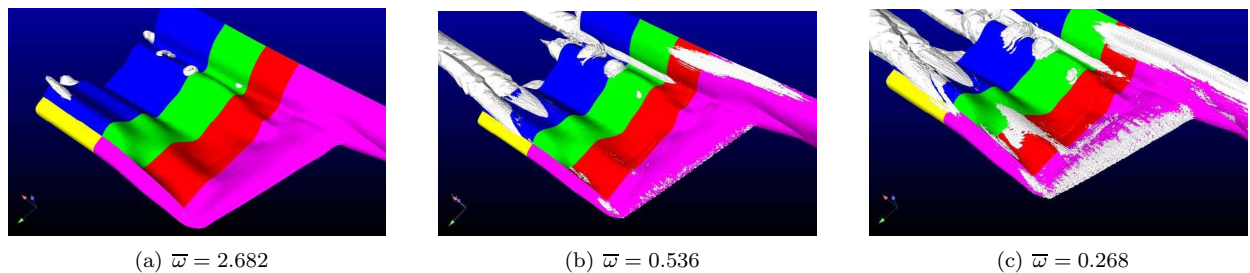| (a) $\overline{\varpi} = 2.682$ | (b) $\overline{\varpi} = 0.536$ | (c) $\overline{\varpi} = 0.268$ |

Figure 4. Three isosurfaces of vorticity magnitude are compared with the integral surface. The isosurfaces are labeled by white, and the other colors indicate the partition parts of the integral surface

IV.   Analysis of the Main Results

IV.A.   Results by the Kirchhoff Method

The sources for the noise generation in the flow field are mostly enclosed by the integral surface, as defined above, and thus the approximate total noise $p'_{total,K}$ can be calculated using the Kirchhoff method, as can its componential terms $p'_{i,K}$. The pressure of the noise is evaluated by the sound pressure level (SPL)

measured in decibels (dB), which is defined by $SPL = 20log_{10}(p'/p_{ref})$. Here the reference pressure, p_{ref}, is 2×10^{-5} Pa. For reasons of confidentiality, the actual amplitudes of the plots in this paper have been removed.

Figure 5 displays the SPL of $p'_{i,K}$ and $p'_{total,K}$ with respect to the Strouhal number, St, at four observers, i.e. $\theta = 0^o$, 90°, 180° and 270°. The Strouhal number is defined as $St = fL/U$, where L is the characteristic length of the chord of the wing and U is the velocity of the freestream. θ is the angle towards the polar axis, which points to the upstream direction. Even though the result at 180° is inaccurate in principle and is uninteresting in practice, as discussed above, it is presented to help future studies. The results at 0° and 90° are shown for the same purpose. They are theoretically correct but not beneficial in practical applications. It is seen that $p'_{1,K}$ related to the pressure perturbations is negligible compared with the other two. This supports the near-field property of the component. As shown in subfigures (b) and (d) of Fig. 5, significant amplitude difference between $p'_{2,K}$ and $p'_{3,K}$ appears for $St < 1.2$, and $p'_{2,K}$ is the highest term. It should be noted that the SPL of $p'_{total,K}$ is obtained by calculating the SPL to the summation of pressures of $p'_{i,K}$. After this calculation treatment, it is difficult to observe influences of the noise from the subdominant terms in the SPL, i.e., $p'_{1,K}$ and $p'_{2,K}$.

The overall sound pressure levels (OASPL) measured in dB are shown in Fig. 6. The polar axis for the OASPL points to the upstream direction. The influences from the first and third terms are insignificant in the OASPL for the same reason as stated for the SPL. The OASPL of $p'_{1,K}$ is drawn separately in Fig. 6(b) because of its small amplitude. It is observed that $p'_{1,K}$ and $p'_{3,K}$ follow the dipole trend, and $p'_{2,K}$ follows the monopole trend. The dipole feature of $p'_{3,K}$ proves that its SPL at 0° shows a different tendency in comparison with 90° and 180°.

IV.B.   Results by the FWH Method

The total noise, $p'_{total,F}$, and its componental terms, $p'_{i,F}$ are computed. The SPL of $p'_{total,F}$ and $p'_{i,F}$ is shown in Fig. 7. $p'_{3,F}$, which is related to $\partial (\rho u_j) / \partial \tau$ of the source, is dominant. As for the Kirchhoff method, the effects of the other two components are negligible in the figure. However, $p'_{1,F}$, connected to the pressure perturbation of the source, and $p'_{2,F}$, connected to $\rho u_i u_j$ of the source, tend towards a different decaying law at 0° and 180° in contrast to 90° and 270°. Figure 8 shows the OASPL of $p'_{total,F}$ and $p'_{i,F}$. It is found that $p'_{1,F}$ is the noise from dipoles. As shown in Eq. (3a), (3c) and (6a), $p'_{1,F}$ corresponds to a summation of $p'_{1,K}$ and $p'_{3,K}$, which are observed to have similar tendencies in the directivities of the dipole in Fig. 6. The noise of $p'_{2,F}$ is also of type of dipole. However, its directive is almost perpendicular to the first term. This results in the SPL of the two terms $p'_{1,F}$ and $p'_{2,F}$ varying in directions, implying that the component $p'_{2,F}$ is uninteresting in practice due to its limited effects in the downwards direction, such as 270°.

IV.C.   Results by the Curle Method

The SPL of the noise at the four observers that are induced by the pressure perturbations on the wall components are plotted individually with respective to St in Fig. 9. The surface of the inboard flap contributes most of the noise in the forward 0° and backward 180° directions. However, differences in amplitudes among all $p'_{i,C}$ are low at 90° and 270°. This phenomenon is illustrated by their OASPL, which are shown in Fig. 10. All components show the dipole property. It is observed, however, that the directivity of the dipole approaches being perpendicular to the incidence angle of the corresponding component surface. The inboard flap is presented as the dominant noise source compared with the other walls in the OASPL.

IV.D.   Numerical Comparison of the Three Methods

To compare the three analogy methods, the SPL of the total sound pressure at four directions are shown in Fig. 11. Here it should be noted that the total pressure computed by the Curle method corresponds to the noise contributed by all walls but not the core flow region, which is included in the other two methods. It is observed that the noise given by the FWH method is highest for $1 < St < 8$, except at 0°. The differences in amplitude between the FWH method and the Kirchhoff methods reflect the effects of the nonlinear source terms that are not involved in the latter method. Furthermore, all SPL decay at the same rate in the frequency band from $St = 8$ to 20. However, those given by the Curle method decay faster than the others at higher St. The discrepancies between the Curle method and the other methods are caused by the effects of the volume sources. Figure 12 shows a comparison of the OASPL given by the three methods. A higher
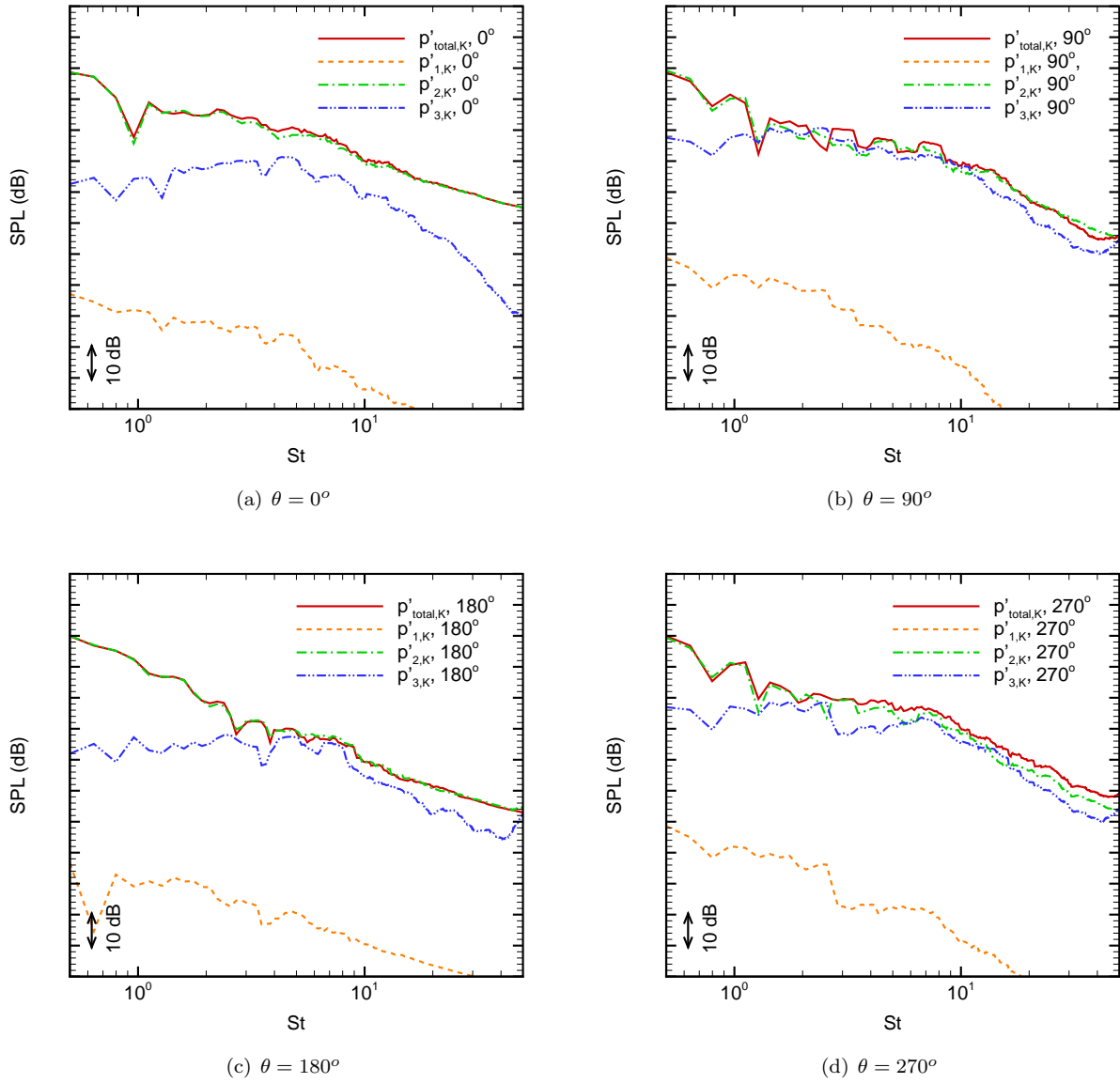
American Institute of Aeronautics and Astronautics Paper 2012-0386

(a) $\theta = 0^o$

(b) $\theta = 90^o$

(c) $\theta = 180^o$

(d) $\theta = 270^o$

Figure 5. SPL given by the Kirchhoff method at four observers

(a) p'_{total}, p'_2 and p'_3
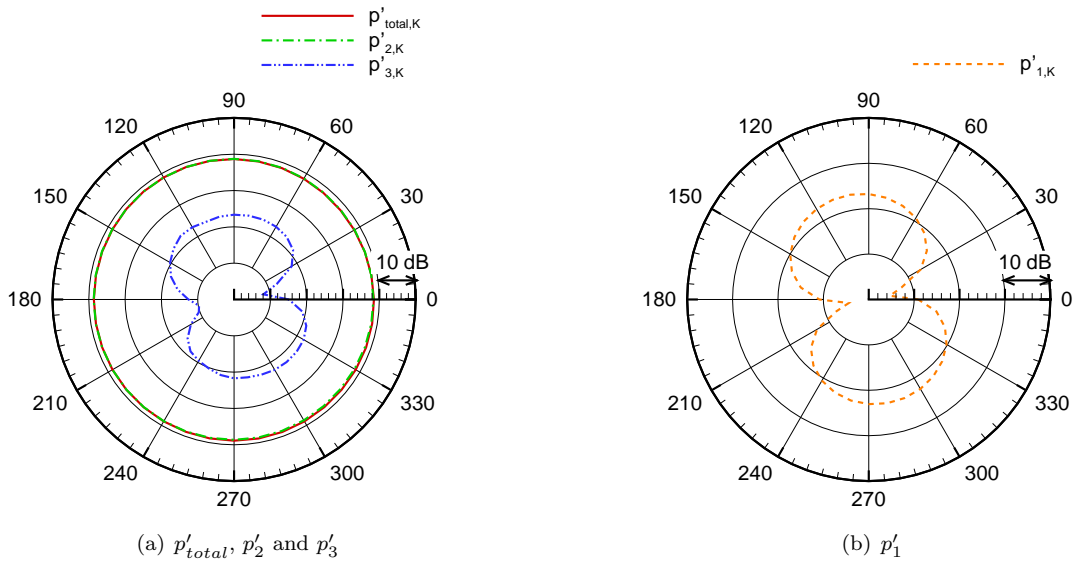
(b) p'_1

Figure 6. OASPL given by the Kirchhoff method for the total sound pressure, $p'_{total,K}$, and its components, $p'_{i,K}$. Here the maximum value for the range of the R-axis in figure b is equal to the minimum value of that in figure a

noise level is predicted by the Kirchhoff method than the FWH method. Results gained with the Curle method show a distinct directivity as compared with the others.

V.   Conclusions

A three-dimensional wing with low-noise and high-lift devices that is referred to as Config. 2 in the companion paper[32] is used to study the acoustic analogy approaches, the Kirchhoff method, the FWH method of the permeable surface and the Curle method. The first two approaches are applied to predict the noise contributed by a common core region of the flow, and the last one is used to predict the noise specifically from the pressure perturbations over the walls. The instantaneous flow field that is used in the analogy approaches is calculated by a hybrid method of RANS and LES.

Due to the complexity of the flow field of the high-lift wing, a way to construct the integral surface following the local flow features is proposed for the Kirchhoff method and the FWH method. Vorticity is chosen as the reference variable for the surface construction. Its estimation is provided by a precursor RANS computation.

The noise predicted by the Kirchhoff method is analyzed on the basis of integrations of the source terms, which include the dependent quantities on the integral surface, i.e. the pressure perturbations, p', its gradient, dp/dn, and its time derivative, dp/dt. It is found that the pressure gradient is the dominant source term. It is close to a monopole source. However, the noise from the pressure and time derivative present dipoles whose strong polar point upwards and downwards.
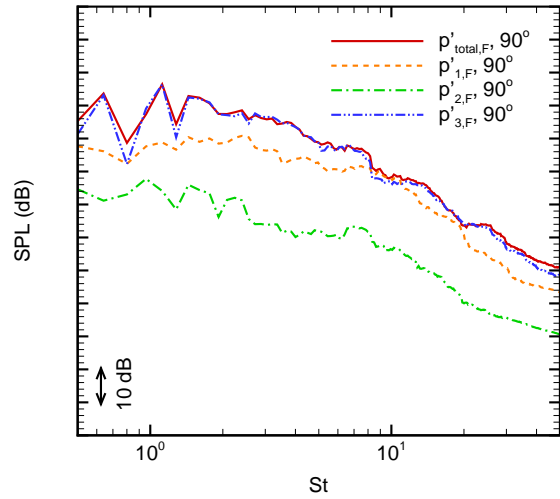
Using the FWH method, the noise can be related to the dependent sources of the variations of the pressure, p', the flow momentum, $\rho u_i u_j$, and the flow mass, ρu_j. The flow mass is found to be the dominant term. It induces the noise with an approximate monopole directivity. The other two components follow the dipoles, but their directivities tend to be perpendicular to each other. The strong polar by the flow momentum points to the downstream and upstream and is thus unimportant in practice.

The Curle method gives the noise induced individually by the fluctuating pressure of the boundary layer over each wall component. The wall of the inboard flap is found to be the dominant source. The radiation directivities of the dipole sources of the pressure are relative to the incidence angles of the wall components.
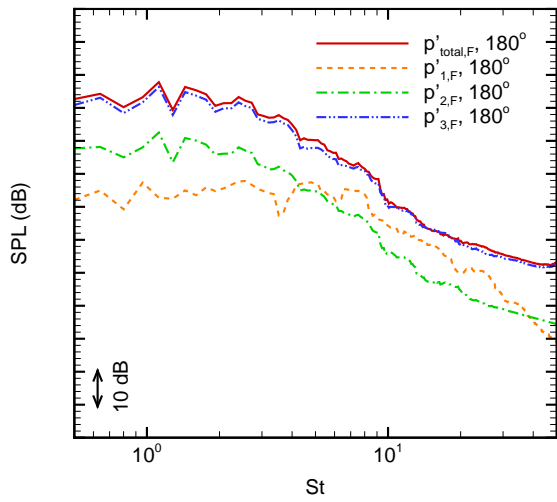
The differences between the noise predicted by the Kirchhoff method and the FWH method appear mainly in the range of $1 < St < 8$. A possible reason is that the nonlinear effect is not involved in the Kirchhoff formulation. Comparing the results given by the Curle method with those given by the other two methods, it is found that the volume sources are important for prediction of the noise from the high-lift wing.
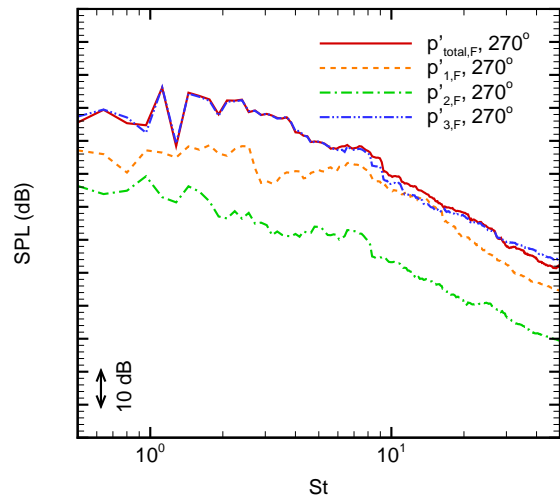
American Institute of Aeronautics and Astronautics Paper 2012-0386

(a) $\theta = 0^o$

(b) $\theta = 90^o$

(c) $\theta = 180^o$

(d) $\theta = 270^o$
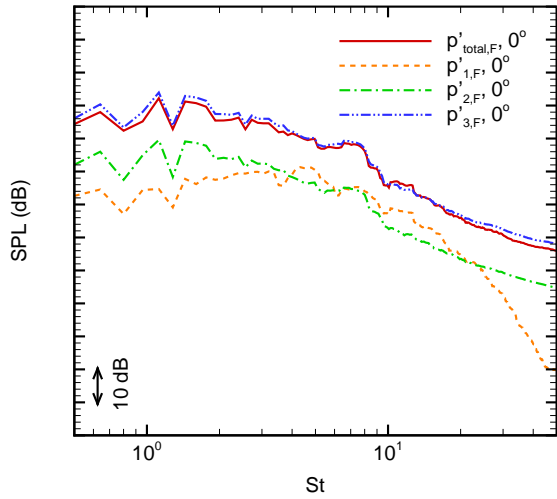
Figure 7. SPL given by the FWH method at four observers

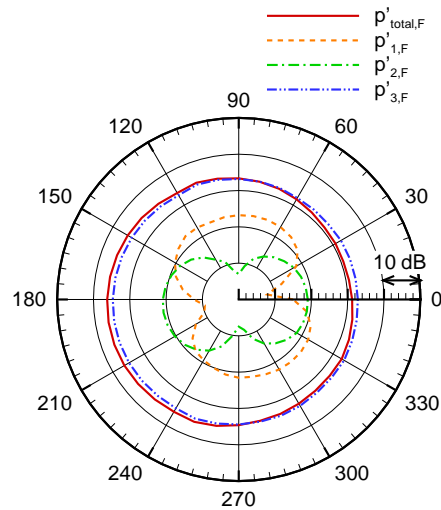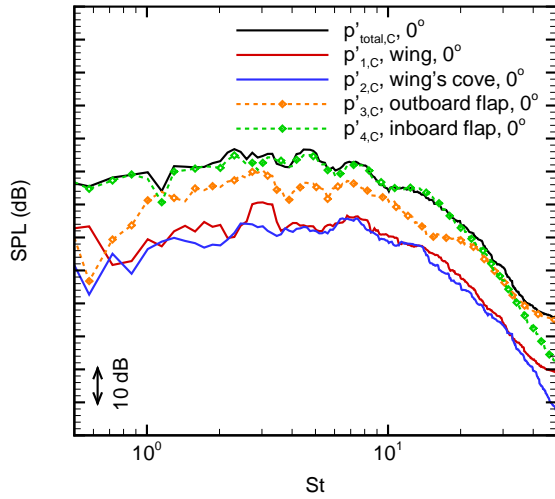**Figure 8. OASPL given by the FWH method for the total sound pressure, $p'_{total,F}$, and its components, $p'_{i,F}$**

Acknowledgments

References

[1]Lighthill, M. J., "On Sound Generated Aerodynamically. I. General Theory," *Proc. Roy. Soc.*, Vol. A 211, 1952, pp. 564–587.

[2]Lighthill, M. J., "On Sound Generated Aerodynamically. II. Turbulence as a Source of Sound," *Proc. Roy. Soc.*, Vol. A 222, 1954, pp. 1–32.

[3]Curle, N., "The Influence of Solid Boundaries Upon Aerodynamic Sound," *Proc. Roy. Soc.*, Vol. A 231, 1955, pp. 505–514.

[4]Williams, J. E. F. and Hawkins, D. L., "Sound Generation by Turbulence and Surfaces in Arbitrary Motion," *Philos. Trans. Roy. Soc.*, Vol. A 264, No. 1151, 1969, pp. 321–342.

[5]di Francescantonio, P., "A New Kirchhoff Formulation for Transonic Rotor Noise," *Journal of Sound and Vibration*, Vol. 202, No. 4, 1997, pp. 491–509.

[6]Brentner, K. S. and Farassat, F., "An Analytical Comparison of the Acoustic Analogy and Kirchhoff Formulation for Moving Surfaces," *AIAA Journal*, Vol. 36, No. 8, 1998, pp. 1379–1386.

[7]Kirhhoff, G. R., "Zur Theorie der Lichtstrahlen," *Annalen der Physik und Chemie*, Vol. 18, 1883, pp. 663–695.

[8]Morgans, R. P., "The Kirchhoff Formula Extended to a Moving Surface," *Philosophical Magazine*, Vol. 9, No. 55, 1930, pp. 141–161.

[9]Farassat, F. and Myers, M. K., "Extension of Kirchhoffs Formula to Radiation from Moving Surfaces," *Journal of Sound and Vibration*, Vol. 123, No. 3, 1988, pp. 451–461.

[10]Farassat, F. and Myers, M. K., "The Kirchhoff Formula for a Supersonically Moving Surface," *First Joint CEAS/AIAA Aeroacoustics Conference*, AIAA 95-062, 1995.

[11]Lyrintzis, A. S., "Review: the Use of Kirchhoff Method in Computational Aeroacoustics," *ASME Journal of Fluids Engineering*, Vol. 116, No. 4, 1994, pp. 665–676.

[12]Freund, J. B., Lele, S. K., and Moin, P., "Caculation of the Radiated Sound Field Using an Opening Kirchhoff Surface," *AIAA Journal*, Vol. 34, No. 5, 1996, pp. 909–916.

[13]Farassat, F., "Acoustic Radiation from Rotating Blades - the Kirchhoff Method in Aeroacoustics," *Journal of Sound and Vibration*, Vol. 239, No. 4, 2001, pp. 785–800.

[14]Brentner, K. S. and Farassat, F., "Modeling Aerodynamically Generated Sound of Helicopter Rotors," *Progress in Aerospace Sciences*, Vol. 39, 2003, pp. 83–120.

[15]Prieur, J. and Rahier, G., "Aeroacoustic integral methods, formulation and efficient numerical implementation," *Aerospace Science and Technology*, Vol. 5, 2001, pp. 457–468.

[16]Lyrintzis, A. S. and Uzun, A., "Integral Techniques for Jet Aeroacoustics Calculations," *7th AIAA/CEAS Aeroacoustics Conference, Maastricht, Netherlands*, AIAA 2001-2253, 2001.

[17]Lockard, D. P. and Lilley, G. M., "The Airframe Noise Reduction Chanllenge," NASA/TM–2004–213013, 2004.

[18]Singer, B. A., Brentner, K. S., Lockard, D. P., and Lilley, G. M., "Simulation of Acoustic Scattering from a Trailing Edge," *Journal of Sound and Vibraion*, Vol. 230, No. 3, 2000, pp. 541–560.
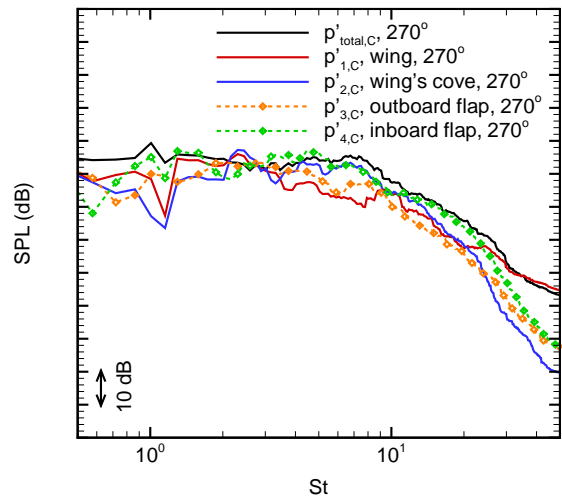
(a) $\theta = 0^o$

(b) $\theta = 90^o$

(c) $\theta = 180^o$

(d) $\theta = 270^o$
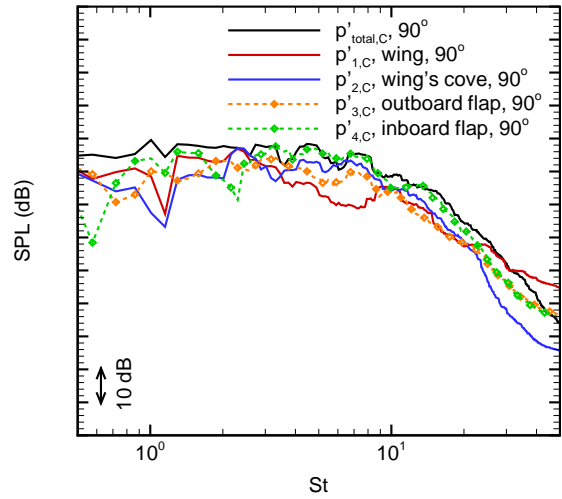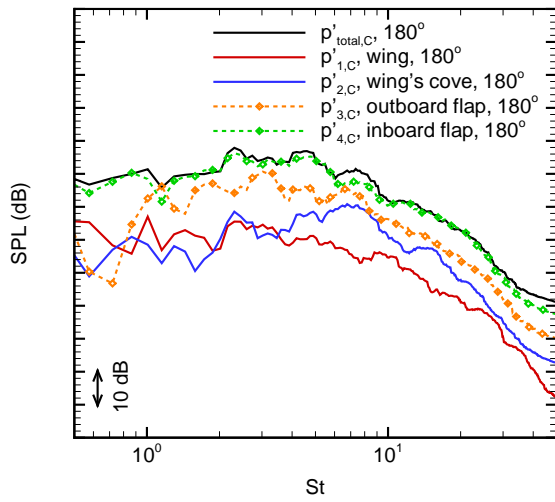
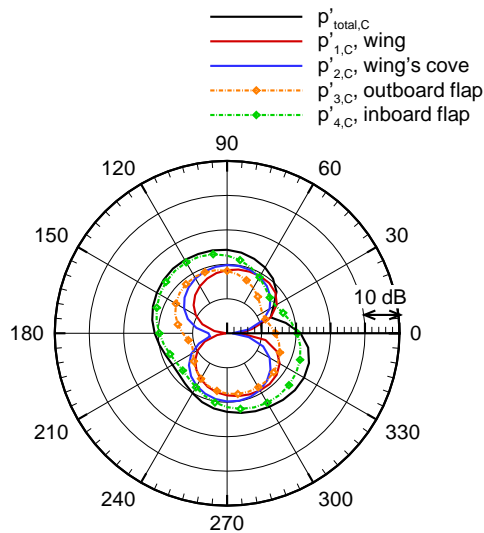Figure 9. SPL given by the Curle method at four observers

Figure 10. OASPL given by the Curle method for the total sound pressure, $p'_{total,C}$, and its components from the walls of the wing, the wing's cove, the outboard flap and the inboard flap

[19]Howe, M. S., "On the Hydroacoustics of a Trailing Edge with a Detached Flap," *Journal of Sound and Vibration*, Vol. 239, No. 4, 2001, pp. 801–817.

[20]Amiet, R. K., "Noise Due to Turbulence Flow Past a Trailing Edge," *Journal of Sound and Vibration*, Vol. 47, No. 3, 1976, pp. 387–393.

[21]Roger, M. and Moreau, S., "Back-Scattering Correction and Further Extensions of Amiet's Trailing-Edge Noise Model. Part 1: Theory," *Journal of Sound and Vibration*, Vol. 286, 2005, pp. 477–506.

[22]Moreau, S. and Roger, M., "Back-Scattering Correction and Further Extensions of Amiet's Trailing-Edge Noise Model. Part 2: Application," *Journal of Sound and Vibration*, Vol. 323, 2009, pp. 397–425.

[23]Tam, C. K. W. and Yu, J. C., "Trailing Edge Noise," *2nd AIAA Aeroacoustics Conference*, AIAA 1975-489, 1975.

[24]Kalitzin, G., Kalitzin, N., and Wilde, A., "A Factorization Scheme for RANS Turbulence Models and SNGR Predictions of Trailing Edge Noise," *21st AIAA Aeroacoustics Conference*, AIAA 2000-1982, 2000.

[25]Ewert, R. and Schröder, W., "On the Simulation of Trailing Edge Noise with a Hybrid LES/APE Method," *Journal of Sound and Vibration*, Vol. 270, 2004, pp. 509–524.

[26]Sandberg, R. D., Jones, L. E., Sandham, N. D., and Joesph, P. F., "Direct Numerical Simulations of Tonal noise Generated by Laminar Flow Past Airfoils," *Journal of Sound and Vibration*, Vol. 320, 2009, pp. 838–858.

[27]Ewert, R., "Broadband Slat Noise Prediction Based on CAA and Stochastic Sound Sources from a Fast Random Particle Mesh (RPM) Method," *Computers and Fluids*, Vol. 37, 2008, pp. 369–387.

[28]Lockard, D. P. and Choudhari, M. M., "Noise Radiation from a Leading-Edge Slat," *15th AIAA/CEAS Aeroacoustics Conference*, AIAA 2009-3101, 2009.

[29]Howe, M. S., "On the Generation of Side-Edge Flap Noise," *Journal of Sound and Vibration*, Vol. 80, No. 4, 1982, pp. 555–573.

[30]Casper, J. H., Lockard, D. P., Khorrami, M. R., and Streett, C. L., "Investigation of Volumetric Sources in Airframe Noise Simulations," *10th AIAA/CEAS Aeroacoustics Conference*, AIAA 2004-2805, 2004.

[31]Singer, B. A., Lockard, D. P., and Brentner, K. S., "Computational Aeroacoustics Analysis of Slat Trailing Edge Flow," *5th AIAA/CEAS Aeroacoustics Conference*, AIAA 99-1802, 1999.

[32]Yao, H. D., Eriksson, L. E., Davidson, L., Grundestam, O., Peng, S. H., and Eliasson, P. E., "Aeroacoustic Assessment of Conceptual Low-Noise High-Lift Configurations," 2012, accepted.

[33]Goldstein, M. E., editor, *Aeroacoustics*, McGraw-Hill Book Company, New York, 1976.

[34]Wagner, C., Hüttl, T., and Sagaut, P., editors, *Large-Eddy Simulation for Acoustics*, Cambridge University, 2007.
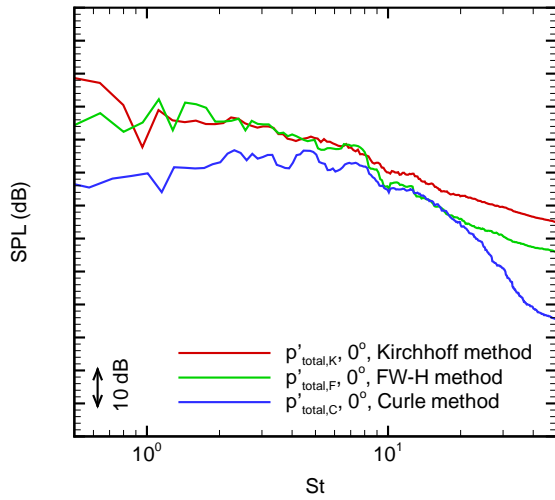
[35]Lyrintzis, A. S., "Surface Integral Methods in Computational Aeroacoustics - from the (CFD) Near-Field to the (Acoustic) Far-Field,," *CEAS Workshop From CFD to CAA*, Athens Greece, 2002.

[36]Andersson, N., Eriksson, L. E., and Davidson, L., "Investigation of an Isothermal Mach 0.75 Jet and its Radiated sound Using Large-Eddy Simulation and Kirchhoff Surface Integration," *International Journal of Heat and Fluid Flow*, Vol. 26, No. 3, 2005, pp. 393–410.
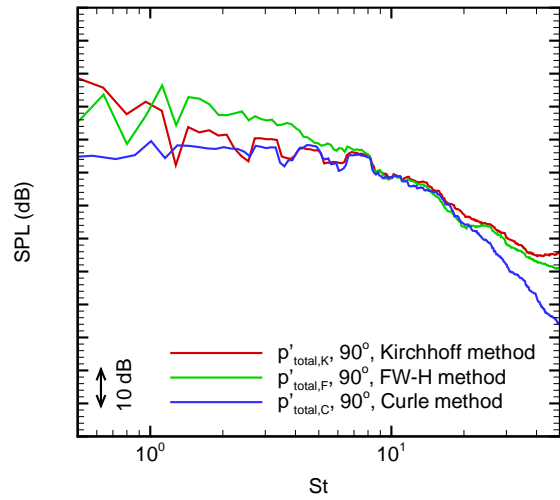
[37]Pan, F. L., Uzun, A., and Lyrintzis, A. S., "Surface Integral Methods in Jet Aeroacoustics: Refraction Corrections," *Journal of Aircraft*, Vol. 45, No. 2, 2008, pp. 381–387.

[38]Manoha, E., Redonnet, S., Delahay, C., Sagaut, P., Mary, I., Khelil, S. B., and Guillen, P., "Numerical Prediction of the Unsteady Flow and Radiated Noise from a 3D Lifting Airfoil," *IRTO AVT Symposium on Ageing Mechanisms and Control: Part A - Developments in Computational Aero- and Hydro-Acoustics*, Manchester, UK, 2001.
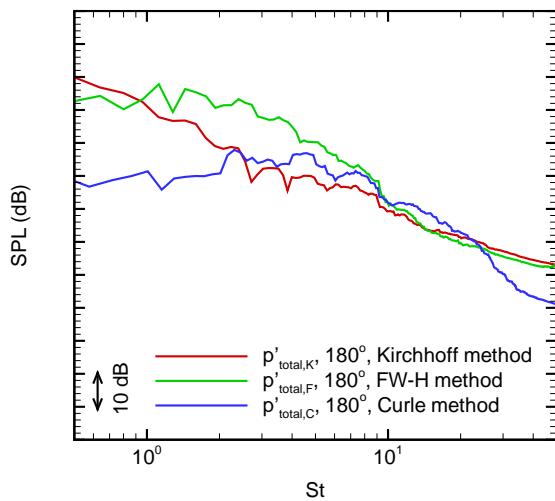
[39]Rahier, G., Prieur, J., Vuillot, F., Lupoglazoff, N., and Biancherin, A., "Investigation of Integral Surface Formulations for Acousitc Predictions of Hot Jets Starting from Unsteady Aerodynamic Simulations," *9th AIAA/CEAS Aeroacoustics Conference*, AIAA 2003-3164, 2003.
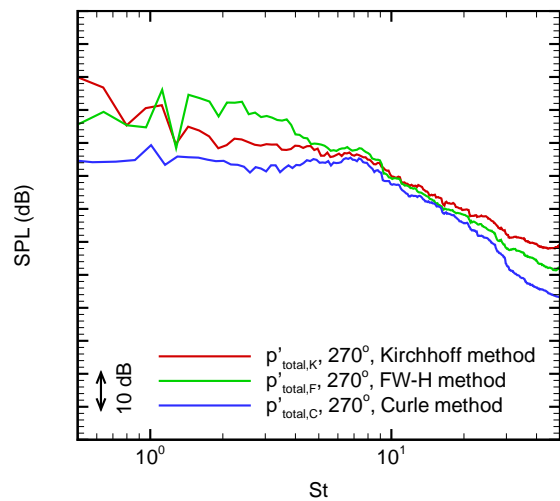
(a) $\theta = 0^o$

(b) $\theta = 90^o$

(c) $\theta = 180^o$

(d) $\theta = 270^o$

Figure 11. SPL of p'_{total} computed by the three methods are compared at four observers

American Institute of Aeronautics and Astronautics Paper 2012-0386

p'total,K, Kirchhoff method
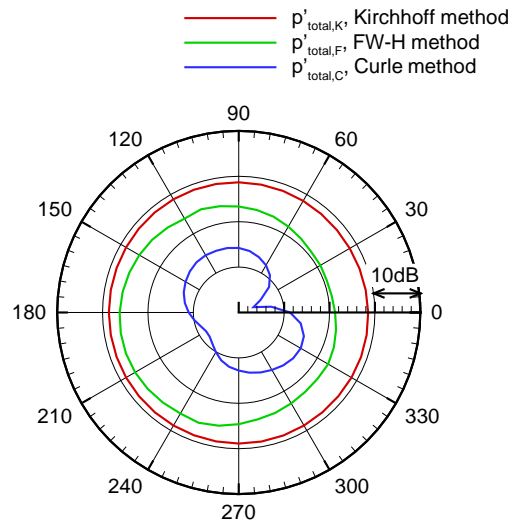p'total,F, FW-H method
p'total,C, Curle method

Figure 12. OASPL of p'_{total} computed by the three methods are compared.

[40] Peng, S. H., "Algebraic hybrid RANS-LES modelling applied to incompressible and compressible turbulent flows," *36th AIAA Fluid Dynamics Conference 4*, AIAA 2674-2690, 2006.

[41] Grundestam, O., Peng, S. H., Eliasson, P. E., Yao, H. D., Davidson, L., and Eriksson, L. E., "Local Flow Properties in Relation to Noise Generation for Low-Noise High-Lift Configurations," *50th AIAA Aerospace Sciences Meeting*, 2012, accepted.